

## Development and Test of Large Size GEM Detectors

S. Bachmann, A. Bressan, A. Placci, L. Ropelewski and F. Sauli  
CERN, Geneva, Switzerland

### Abstract

We discuss the main operating features of GEM detectors, optimized for use as trackers in a high radiation environment. The construction, tests and performances of large prototypes for the COMPASS experiment are also described, as well as the results of an exposure to very high intensity beams.

### I. GEM OPERATION AND PERFORMANCES

The basic element in GEM detectors is a thin polymer foil, metal-clad on both sides, pierced by a high density of holes [1]. On application of a difference of potential between the two electrodes, electrons released by radiation in the gas on one side of the structure are drifted into the holes, multiplied and released on the second side. The multiplier can be used as detector on its own; installed however as pre-amplifying element in front of another micro-pattern device, it permits to reach larger overall gains in harsh radiation environments [2-4]. With two GEM in cascade, the electron charge can directly be detected on a segmented printed circuit, see Fig. 1 [5]. With a special two-levels read-out board, two-dimensional localization can be performed with both electrodes kept at ground potential, a considerable practical advantage [6].

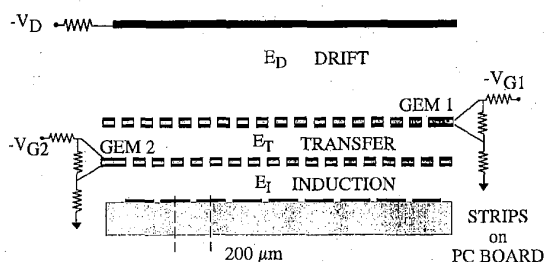


Figure 1: Schematics of the double-GEM detector with 2-D PCB readout.

Performances of double-GEM detectors have been extensively studied both in the laboratory and in test beams. The most relevant are a position resolution for minimum ionizing tracks, perpendicular to the detector, of 40  $\mu\text{m}$  rms, and a time resolution of 18 ns fwhm. The achievable gain at moderate radiation fluxes is as large as  $10^5$ , whilst it still exceeds  $10^4$  at high rates, above  $10^5 \text{ mm}^{-2}\text{s}^{-1}$  (Fig. 2). This holds also when exposing the detector to strongly ionizing particles [7, 8]. Given the value of gain, a few thousand, needed for efficient detection of fast particles with existing electronics, a sufficient margin for proper operation is obtained, ensuring a comfortable efficiency plateau for minimum ionizing particles, even in presence of highly ionizing background.

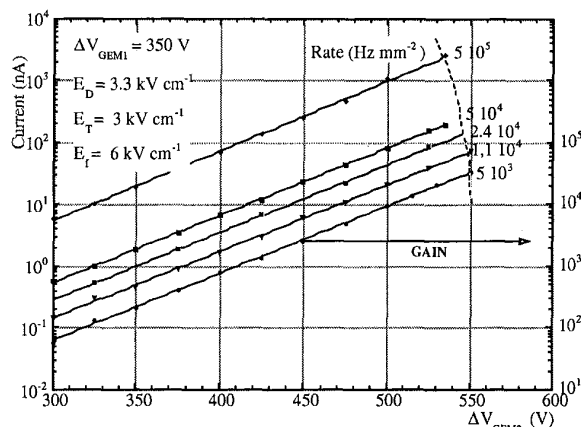


Figure 2: Current in the double GEM detector as a function of voltage and increasing x-ray fluxes. The value of gain can be read on the right scale for the lowest curve.

A gas mixture of argon and  $\text{CO}_2$  in the volume proportion 70-30 has been used in the present work. Although not the best for obtaining the highest gain, it has the advantage to be not flammable, chemically stable and with a fast electron drift velocity; it is also intrinsically non-aging under heavy avalanche conditions. A stable gain under high rate, long-term exposure to radiation has been demonstrated with a double-GEM detector operated with this gas mixture, see Fig. 3 [9], even using a conventional fiberglass-epoxy assembly technology, banned for the more susceptible gas micro-strip chambers. Notice in the figure that a single wire counter installed in the same gas line for monitoring purposed did show instead signs of aging.

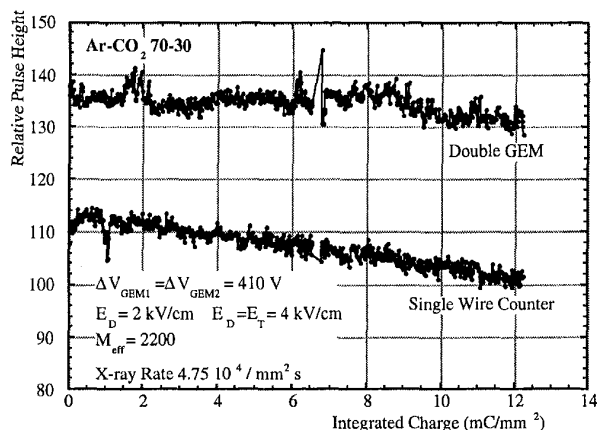


Figure 3: Long-term gain stability under irradiation. A single-wire counter in the same gas line shows aging.

## II. THE COMPASS PROTOTYPES

The major requirements for the COMPASS tracking detectors, in construction at CERN, are a compact structure with low mass, and the largest possible ratio of active to total surface. Two-dimensional read-out obviously helps reducing the number of detectors and their mass. A dead area with the size of the beam spot in the center of the detectors is needed to avoid occupancy problems in the high intensity runs. The design adopted is shown schematically in Fig. 4. The main components of the detector are two identical GEMs with an active surface of  $31 \times 31 \text{ cm}^2$ , a projective two-coordinate read-out printed circuit board (PCB), and a drift electrode delimiting the sensitive volume. Both GEMs and PCB are manufactured on  $50 \mu\text{m}$  thick kapton, clad on both sides with a  $5 \mu\text{m}$  copper layer, with technologies developed in the CERN workshops<sup>1</sup>. For the GEMs, we have adopted a standard high gain design, with regularly spaced  $70 \mu\text{m}$  holes in hexagonal patterns at a  $140 \mu\text{m}$  pitch [10]. In order to keep the overall mass of the detector at minimum inside and outside the active area, we have used two light honeycomb plates, 3 mm thick, as supporting structures, and very thin (5 mm wide) frames for the detector assembly. The resulting thickness in the active area is below 3‰ of a radiation length for each pair of coordinates.

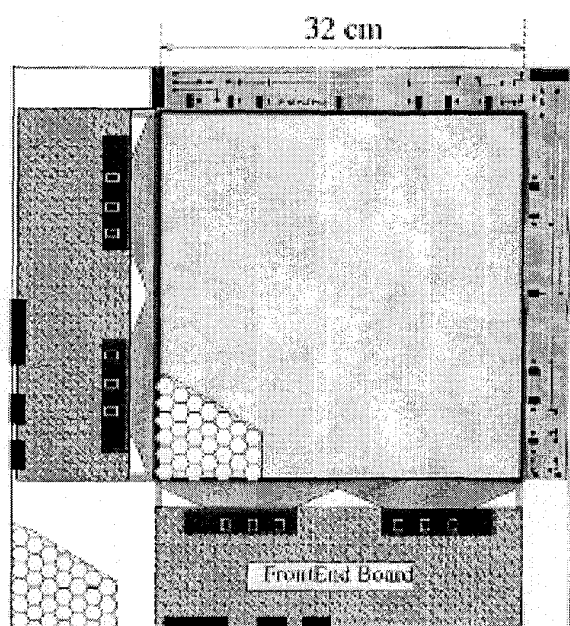


Figure 4: Schematics of the COMPASS prototype. The active area is  $31 \times 31 \text{ cm}^2$ .

To decrease the total energy in case of discharges, one electrode in each GEM is segmented into four sectors connected to the common high voltage line via individual protection resistors. An inner disk, 5 cm in diameter, is independently powered through a thin insulated line running along the center of the electrode (Fig. 5). Decreasing the

voltage difference in this region prevents detection of the beam; the region can be however activated in low intensity runs, to ease the alignment procedures. Narrow gaps between segments,  $\sim 200 \mu\text{m}$ , minimize efficiency losses but are wide enough to sustain the potential difference necessary to inhibit operation in each sector in case of problems (around 400 V).

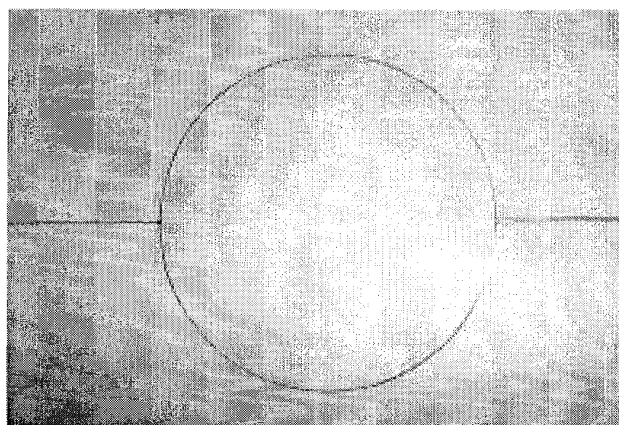


Figure 5: The central GEM partition, independently powered for active control of the beam detection.

The readout board consists of two insulated perpendicular sets of 780 read-out strips each, 31 cm long, with  $400 \mu\text{m}$  pitch, separated by  $50 \mu\text{m}$  thick kapton ridges. In order to achieve uniform sharing of the signals in the two projections, the upper strips have a width of  $80 \mu\text{m}$ , while the lower ones are  $350 \mu\text{m}$  wide. High-density, fast amplifiers cards followed by charge-encoding electronics are wire-bonded on each strip to record the pulse profiles. A three mm thick primary ionization volume has been adopted, a common choice for fast micro-pattern detectors in order to minimize the collection time without loss of efficiency. The one mm gaps between the two GEMs, and between the second GEM and PCB are a compromise between the minimum distance required to effectively separate the two amplification structures, and a reduction of electron diffusion during the drift between elements. Further studies, not completed at the time of the design, suggest that a wider transfer gap (2 mm) is more effective to prevent the propagation of accidental discharges throughout the all structure.

Since the field in the GEM holes dominantly determines the gain, the tolerance in the distance between the different elements of the chamber is not a critical parameter. It affects however the charge transfer efficiency: a 10% variation in the gap results roughly in the same variation in the signal, acceptable for tracking applications. Although the honeycomb support increases the rigidity of the thin frames, high mechanical stress could not be put on the structure without introducing deformations. The use of spacers appeared therefore mandatory in our structures. Several alternatives have been tested in the laboratory on smaller prototypes, before implementation in the larger devices. Between them, thin kapton strips, one mm high, glued to the electrodes in a spiral shape (Fig. 6), one-mm diameter acetate spheres, and epoxy-glass grids with a pitch between 5 and 10 cm and a wall width

<sup>1</sup> Developed by A. Gandi and R. De Oliveira, EST-MT

of  $\sim 400 \mu\text{m}$ , Fig. 7 [11]. To fix the kapton strip and the acetate sphere on the electrodes, we have used two-component epoxy with very good insulating properties. For the grid, a thin layer of glue has been deposited on the plate before machining the grid, and the adhesion was obtained by lamination at high temperature<sup>1</sup>. No degradation in the detector performances due to the spacers has been observed in all three cases, and the only effect is a small inefficient region around the spacer itself. The expected integral efficiency loss induced by the kapton strip and the spheres is very small (0.1 %), while it is larger but still tolerable (1%) for a grid having a pitch of 8 cm. The kapton spiral spacer has been adopted for the first COMPASS detectors; although rather laborious to install, it proved very effective in preventing deformation of the gaps, as demonstrated by the good measured uniformity of gain.

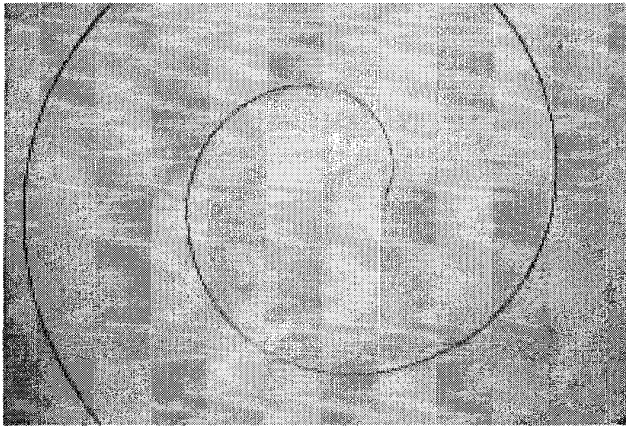


Figure 6: The kapton spiral spacer used to maintain the gap between electrodes constant.

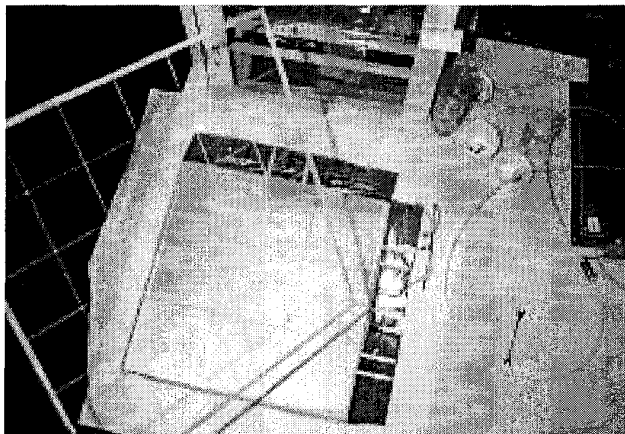


Figure 7: An alternative machined fiberglass spacer.

### III. FIRST RESULTS OF PROTOTYPE TESTING

Two full size prototypes as described have been completed and partly tested so far; the picture in Fig. 8 shows a completed detector. The high voltage to each electrode is supplied to the sectors through individual protection resistors, mounted on distribution boards (top and left in the picture); on each GEM,

the central area (beam killer) is connected to a separate power supply to control the local efficiency. For the initial tests, we have only equipped 128 adjacent strips in each plane with fast analogue readout electronics; all the strips are however connected to ground, making the whole area of the detector active.

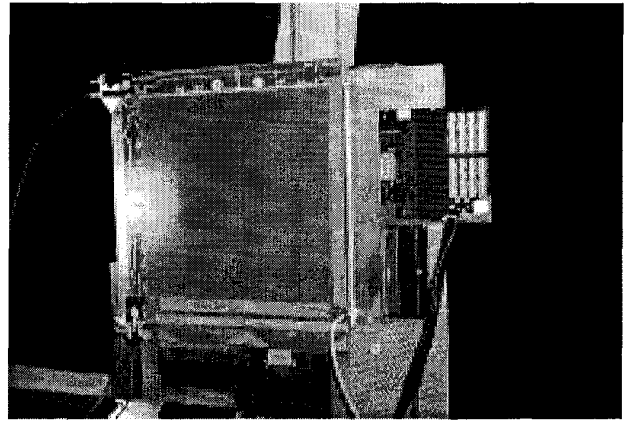


Figure 8: A COMPASS double-GEM prototype, partly equipped with read-out electronics.

Fig. 9 shows the uniformity of gain across the sensitive area, recorded in the first prototype on a group of 16 adjacent strips, using a charge amplifier and a 6 keV X-ray source, at a gain of a few thousand. The second prototype, made with better quality GEMs, could hold safely the nominal voltage required to reach the middle of the efficiency plateau for minimum ionizing particles (420 V on each GEM). Installed in a high intensity beam at CERN, it is at present undergoing systematic tests of reliability and performances.

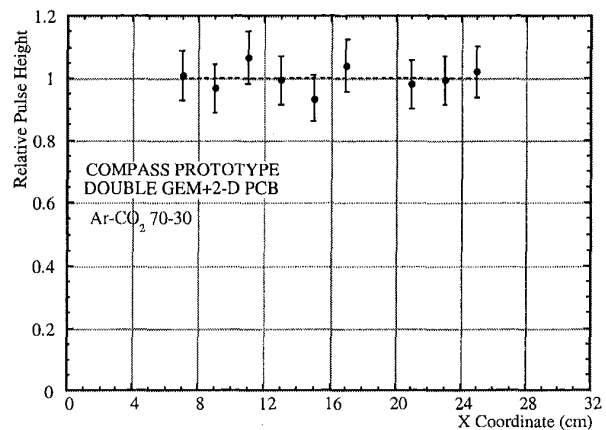


Figure 9: Gain uniformity along one coordinate.

Fig. 10 show the integral pulse height spectra (or cluster charge) recorded on the read-out planes; the small peak on the left represents the electronics noise. The signal over noise ratio is around 40. Fig. 11 is a scatter plot of the charge recorded on one coordinate as a function of the other, showing the excellent correlation between the two projections. This will greatly help finding the correct pairs in multi-prong events.

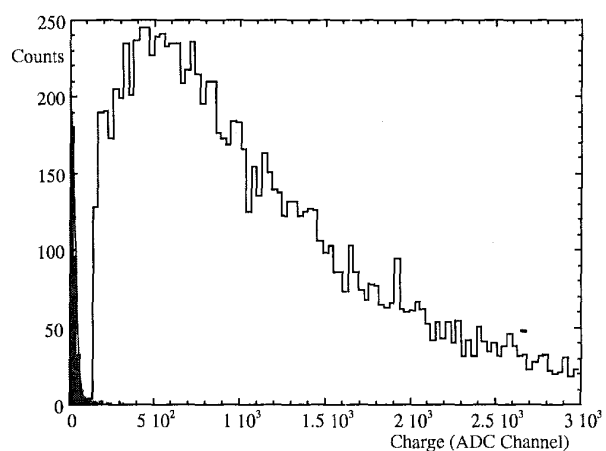
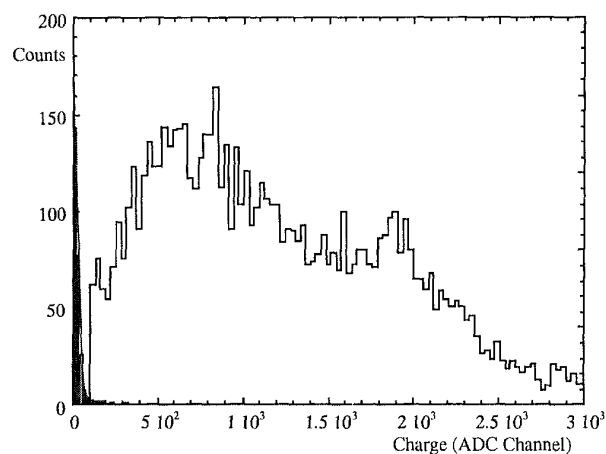


Figure 10: Cluster charge for minimum ionizing particles recorded on the two perpendicular coordinates.

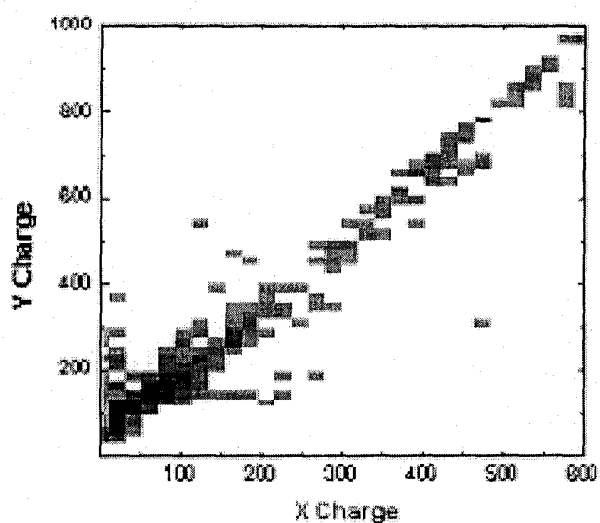


Figure 11: Cluster charge correlation between the two projective coordinates.

The detector has been exposed for several weeks to a high energy charged particle beam at CERN (M2 in the North Hall), firstly at moderate intensities for the gain studies and then to the full intensity expected for the COMPASS experiment. Both voltage scans and medium term continuous exposures have been made. With the exception of a slightly weaker sector in one GEM (probably due to some epoxy accidentally diffused in the holes), all the detector, including the central beam region, could be operated for several days at an effective gain of  $1.2 \cdot 10^4$ , well above the one required for full efficiency. The detector did not produce any discharge when running with the full muon beam ( $10^8$  particles per second), while on the hadron beam ( $10^7$  per second) we recorded an average discharge rate of less than one per hour. Notice that the detector structure is sturdy enough to resist to repeated discharges, and there was no sign of physical damage to the chamber after the irradiation. As this might not apply to the readout electronics, methods of reducing even further the discharge probability, as well to prevent the propagation to the readout board are being studied intensively in the laboratory.

#### IV. REFERENCES

- [1] F. Sauli, Nucl. Instrum. and Meth. vol A386, pp. 531-534, 1997.
- [2] R. Bouclier, W. Dominik, M. Hoch, J. C. Labbé, G. Million, L. Ropelewski, F. Sauli, A. Sharma, G. Manzin, Nucl. Instrum. and Meth. A396, 1997, pp 50-66.
- [3] B. Schmidt, Nucl. Instrum. and Meth., vol. A 419, 1998, pp. 230-238.
- [4] W. Beaumont, T. Beckers, J. DeTroy, V. Van Dyck, O. Bouhali, F. Udo, C. VanderVelde, W. Van Doninck, P. Vanlaer, V. Zhukov, Nucl. Instrum. and Meth., vol. A 419, 1998, pp. 394-401.
- [5] A. Bressan, J. C. Labbé, P. Pagano, L. Ropelewski, F. Sauli, Nucl. Instrum. and Meth., vol. A425, 1999, pp. 262-276.
- [6] A. Bressan, L. Ropelewski, F. Sauli, D. Mörmann, T. Müller, H. J. Simonis, Nucl. Instrum. and Meth., vol. A425, 1999 pp. 254-261.
- [7] A. Bressan, M. Hoch, P. Pagano, L. Ropelewski, F. Sauli, S. Biagi, A. Buzulutskov, M. Gruwé, A. Sharma, D. Moermann, G. De Lentdecker, Nucl. Instrum. and Meth., vol. A424, 1998 pp. 321-342.
- [8] P. Fonte and V. Peskov, Nucl. Instrum. And Meth. A416, 1998, pp.23-31.
- [9] S. Bachmann, A. Bressan, L. Ropelewski, F. Sauli, A. Sharma, A. Sokolov, Proc. Micro-Pattern Gas Detectors Workshop, Orsay, 1999, pp. 61-64.
- [10] J. Benlloch, A. Bressan, M. Capeáns, M. Gruwé, M. Hoch, J. C. Labbé, A. Placci, L. Ropelewski, F. Sauli, Nucl. Instrum. and Meth., vol. A 419, 1998 pp. 410-417.
- [11] S. Bachmann, A. Bressan, A. Placci, L. Ropelewski, and F. Sauli, Proc. Micro-Pattern Gas Detectors Workshop, Orsay, 1999, pp. 83-86.